

miniTAO/ANIR Pad Survey of Local LIRGs

Ken Tateuchi¹ (Email: tateuchi@ioa.s.u-tokyo.ac.jp),

Kentaro Motohara¹, Hidenori Takahashi¹, Natsuko Kato¹, Yuka K.Uchimoto²,

Koji Toshikawa¹, Ryou Ohsawa³, Yuzuru Yoshii¹, Mamoru Doi¹, Kotaro Kohno¹, Kimiaki Kawara¹, Masuo Tanaka¹, Takashi Miyata¹,

Toshihiko Tanabe¹, Takeo Minezaki¹, Shigeyuki Sako¹, Tomoki Morokuma¹, Yoichi Tamura¹, Tsutomu Aoki^{1,4}, Takeo Soyano^{1,4},

Ken'ichi Tarusawa^{1,4}, Shintaro Koshida¹, Takafumi Kamizuka¹, Tomohiko Nakamura¹, Kentaro Asano¹,

これは3にいれるべきですか?

1. Introduction

- Star forming rate (SFR) densities at high redshifts are dominated by infrared bright galaxies (e.g., Goto et al. 2010).
- ~~especially Luminous Infrared Galaxies (LIRGs; $L_{\text{IR}} = L_{[8-1000 \mu\text{m}]} = 10^{11-12} L_{\odot}$) and Ultra Luminous Infrared Galaxies (ULIRGs; $L_{\text{IR}} = 10^{12-13} L_{\odot}$)~~

In order to know the detailed properties of these galaxies, and understand how formed and evolved, spatially resolved information are required.

Local U/LIRGs is an ideal laboratory for spatially resolved star-forming processes.

- U/LIRGs are affected by a large amount of dust extinction (LIRGs; $\text{Av} \sim 3 \text{mag}$, Alonso-herrero et al. 2006), produced by their active star formation activities.
- Because of its relative insensitivity to dust extinction, $\text{Pa}\alpha$ (1.8751 μm ; hydrogen emission line) represents a nearly unbiased tracer of the current SFR

However, it is strongly affected by atmospheric absorption, there are few ground-based observations using the line emission. The goal of this paper is to reveal the properties of U/LIRGs, especially SFR and profile of star forming regions using $\text{Pa}\alpha$.

3. miniTAO / Atacama Near InfraRed Camera



FIG.1 ANIR mounted on the Cassegrain focus of miniTAO telescope

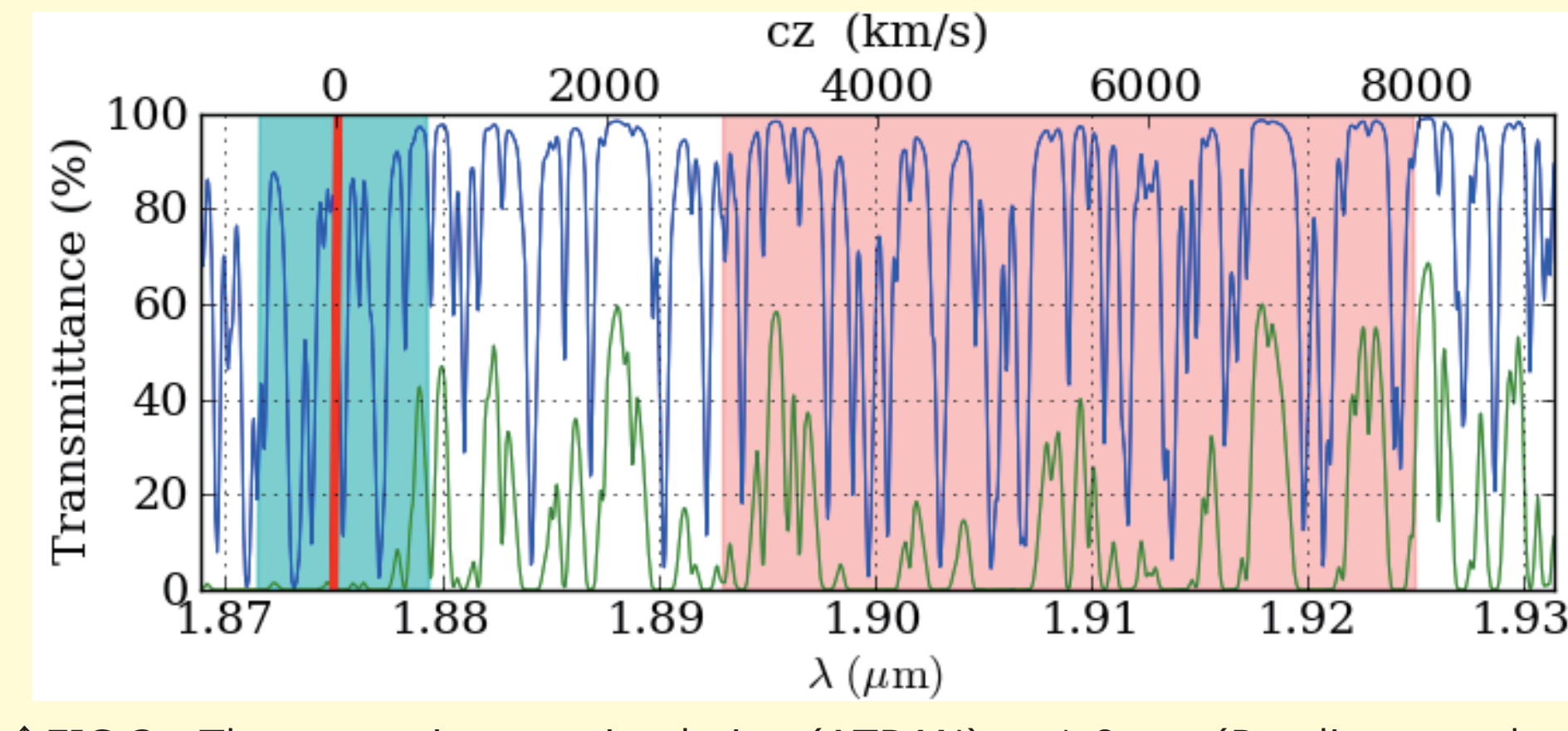


FIG.3 The transmittance simulation (ATRAN) at 1.9 μm (Pad line wavelength region). Blue line is PAO site (5640m; averaged PWV~0.5 mm), and green line is VLT site (2600m; averaged PWV~0mm). Blue area represents the N1875 NB filter, and red area represents the N191 NB filter.

ANIR (Atacama Near InfraRed camera)

A near infrared camera for the University of Tokyo Atacama 1.0m telescope (miniTAO), installed at the summit of Co. Chajnantor (5640m altitude) in northern Chile.

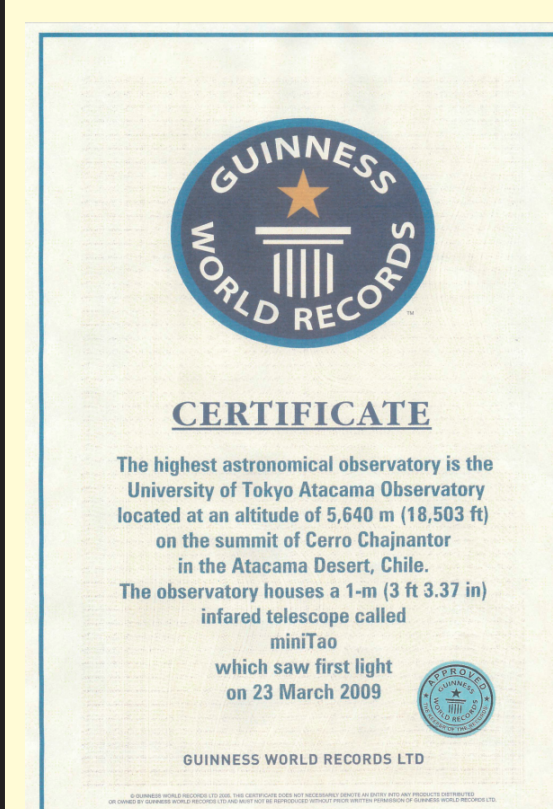


FIG.2 miniTAO located at an altitude of 5640m (18503 ft) is the highest astronomical observatory in the world. The first light observation was carried out in July 2009, and $\text{Pa}\alpha$ images have been successfully obtained using N1875 and N191.

Wavelength	0.85-2.5 μm
Detector	PACE-HAWAII2
Pixel format	1024 x 1024
Pixel pitch	18.5 μm
Readout noise	< 15 e r.m.s. (CDS)
Field of view	5'.25 x 5'.25
Pixel scale	0'.308 pixel ⁻¹
Broad-band Filters	Y,J,H,Ks (MKO filter set)
Narrow-band Filters	N128(PaB), N131(PaB-off), N1875(Paα), N191(Paα-off), N207(CIV)

The high altitude and extremely low precipitable water vapor (PWV=0.5mm) of the site enable us to perform observation of $\text{Pa}\alpha$ (1.8751 μm).

5. Star Forming Rate derived using $\text{Pa}\alpha$

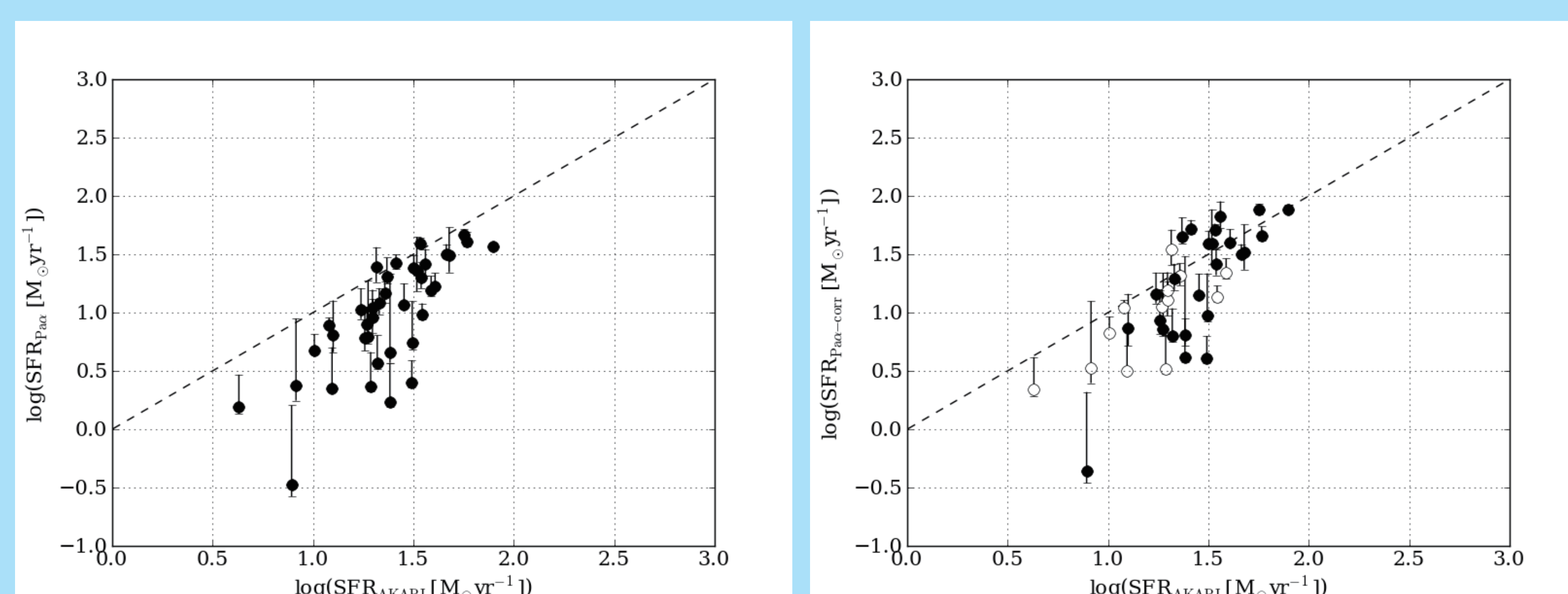


FIG.6 Comparison of the SFRs derived using the infrared obtained by AKARI and $\text{Pa}\alpha$. The SFRs of dust extinction ~~non-corrected~~ $\text{Pa}\alpha$ is left figure and right figure is SFRs of dust extinction ~~corrected~~ $\text{Pa}\alpha$ (Cardelli et al. (1989) dust extinction model is used). White circles in right figure represent that the amounts of dust extinction is assuming $E(B-V)=0.83$ uniform (median amount of dust extinction of IR-galaxies using optical slit spectroscopy (Kim et al. 1995)).

① The AKARI FIR luminosity (Takeuchi et al. 2010)

$$L_{\text{AKARI}} \equiv \Delta v(N60)L_{\nu}(65\mu\text{m}) + \Delta v(WIDE-S)L_{\nu}(90\mu\text{m}) + \Delta(WIDE-L)L_{\nu}(140\mu\text{m})$$

$$\log L_{\text{IR}} = 0.940 \log L_{\text{AKARI}} + 0.914$$

② The relation between SFR and Luminosity (Kennicutt et al. 1998, Rieke et al. 2009)

$$\text{SFR} (M_{\odot} \text{ yr}^{-1}) \equiv 4.5 \times 10^{-44} L_{\nu} [8-1000\mu\text{m}] (\text{erg s}^{-1})$$

$$\text{SFR} (M_{\odot} \text{ yr}^{-1}) \equiv 6.2 \times 10^{-41} L(\text{Pa}) (\text{erg s}^{-1})$$

Left figure of FIG.6 :

the relation between SFRs(IR) and SFRs($\text{Pa}\alpha$ -non-corrected) is good correlation. The median of SFRs($\text{Pa}\alpha$ -non-corrected)/SFRs(IR) is about 0.5, and it shows that it is possible to be good starforming indicator without correcting dust extinction.

Right figure of FIG.6 :

In this figure, dust extinction corrected SFR($\text{Pa}\alpha$) are used. The correction method we used is Balmer line ratio $\text{H}\alpha/\text{H}\beta$. This figure shows that the relation between SFRs(IR) and SFRs($\text{Pa}\alpha$ -corrected) is better correlation. However, for some galaxies, SFRs($\text{Pa}\alpha$) are lower than SFRs(IR) by an order of magnitude.

This suggests that the correction for dust extinction estimated in optical wavelengths is insufficient due to huge amount of dust in those galaxies.

7. SUMMARY

- 38 objects were obtained by miniTAO/ANIR with $\text{Pa}\alpha$ NB filter imaging.
- A new method to restore $\text{Pa}\alpha$ flux from ground-based observations with a NB filter have been developed.
- For some galaxies, SFRs($\text{Pa}\alpha$ -corrected) are lower than SFRs(IR) by an order of magnitude. It suggests that the correction for dust extinction estimated in optical wavelengths is insufficient due to huge amount of dust in those galaxies.
- We find that LIRGs have two starforming mode
- In these two modes, as the SFR is increased, the value of CL is increased. This trend suggests that there is a star forming region profile connection between LIRGs and ULIRGs.

2. Sample selection

- Sample catalog of IR-galaxies is AKARI/FIS-PSC
- Jun 2009 - Oct. 2011 (5 times observation run)
- Narrow-band (NB) filter imaging
 - Filters: N191(NB filter imaging for redshifted $\text{Pa}\alpha$), H,Ks (broad-band imaging for continuum)
 - Exposure time : about 1h per one set (N191,H,Ks)
 - 9 points dithering observation
- 38 objects are observed (LIRGs:33, non-LIRGs:5)
 - 2800 km/s ~ 8100 km/s (Limited wavelength range of N191 NB filter)
 - $4.5 \times 10^{10} \leq L_{\text{IR}}(8-1000\mu\text{m}) [L_{\odot}] \leq 6.5 \times 10^{11}$

4. Data reduction & Flux Calibration

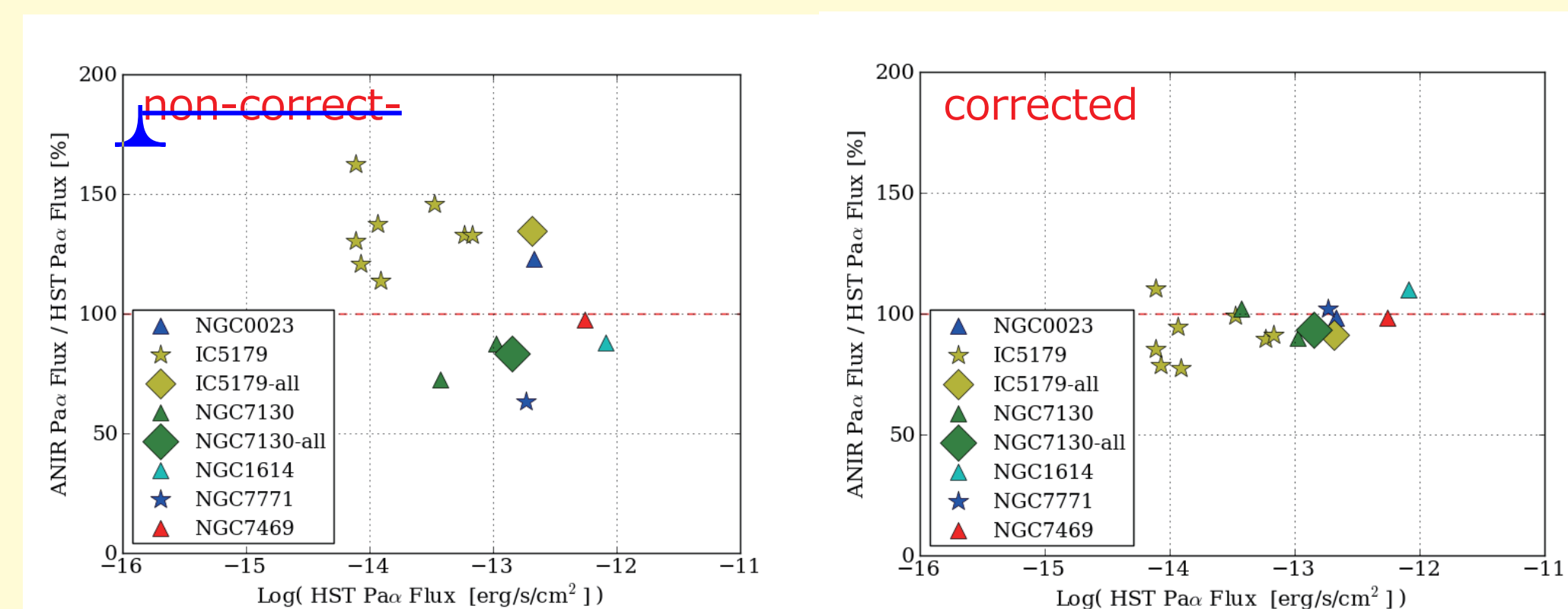


FIG.4 X axis is $\text{Pa}\alpha$ flux obtained by HST/NICMOS, and y-axis is the ratio of the flux obtained by HST/NICMOS to miniTAO/ANIR. Atmospheric absorption ~~non-corrected~~ $\text{Pa}\alpha$ flux of miniTAO/ANIR is left figure, and right figure is atmospheric absorption corrected flux.

It is difficult to calibrate the emission line flux accurately, as there are many atmospheric absorption features within the wavelength range of the narrow-band filters (see FIG.3 please) and they vary temporally due to change of PWV.

In this paper, We have developed a new method to restore $\text{Pa}\alpha$ flux from ground-based observations with a NB filter using model atmosphere by ATRAN (Lord,S.D., 1992)

we were successful in estimating the line emission strength about 10% accuracy relative to other observations from space telescope (HST/NICMOS) (Tateuchi et al. in prep.).

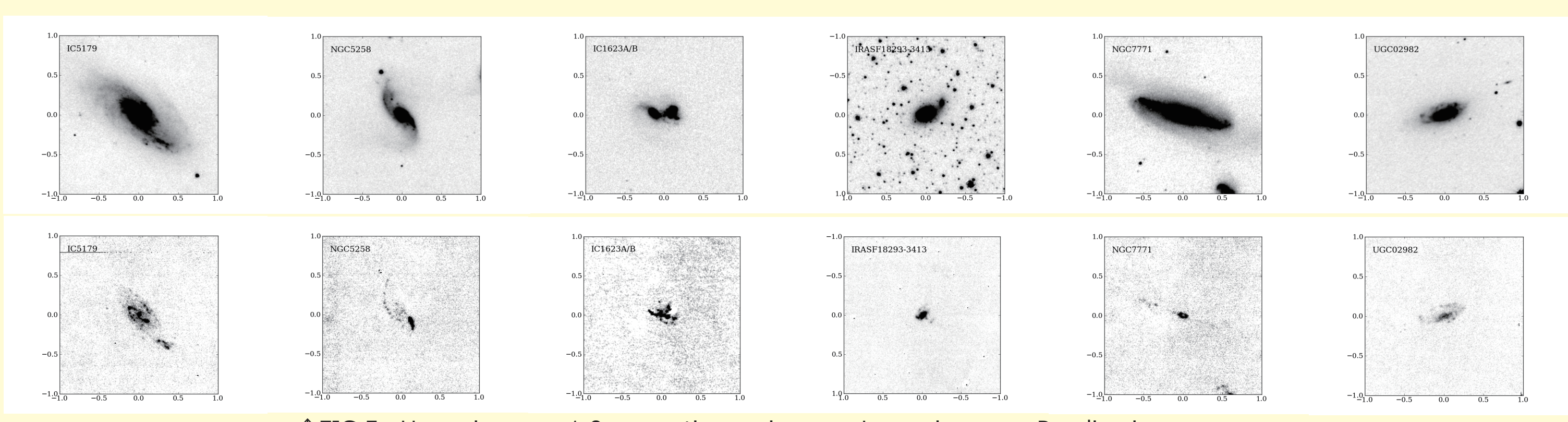


FIG.5 Upper images: 1.9 μm continuum images, Lower images : $\text{Pa}\alpha$ line images

6. Star forming region profile of local LIRGs

To evaluate quantity of star forming region profile of local LIRGs, concentration index (Conselice et al. 2003) are used.

$$C = 5 \log (r_{80}/r_{20})$$

r_{80} : the radii which contain 80% of the total flux

r_{20} : the radii which contain 20% of the total flux

The total flux : 1.5 times the radius Petrosian

C_L : C-Index of starforming regions (Pad line)

C_C : C-Index of stellar population (1.9 μm continuum)

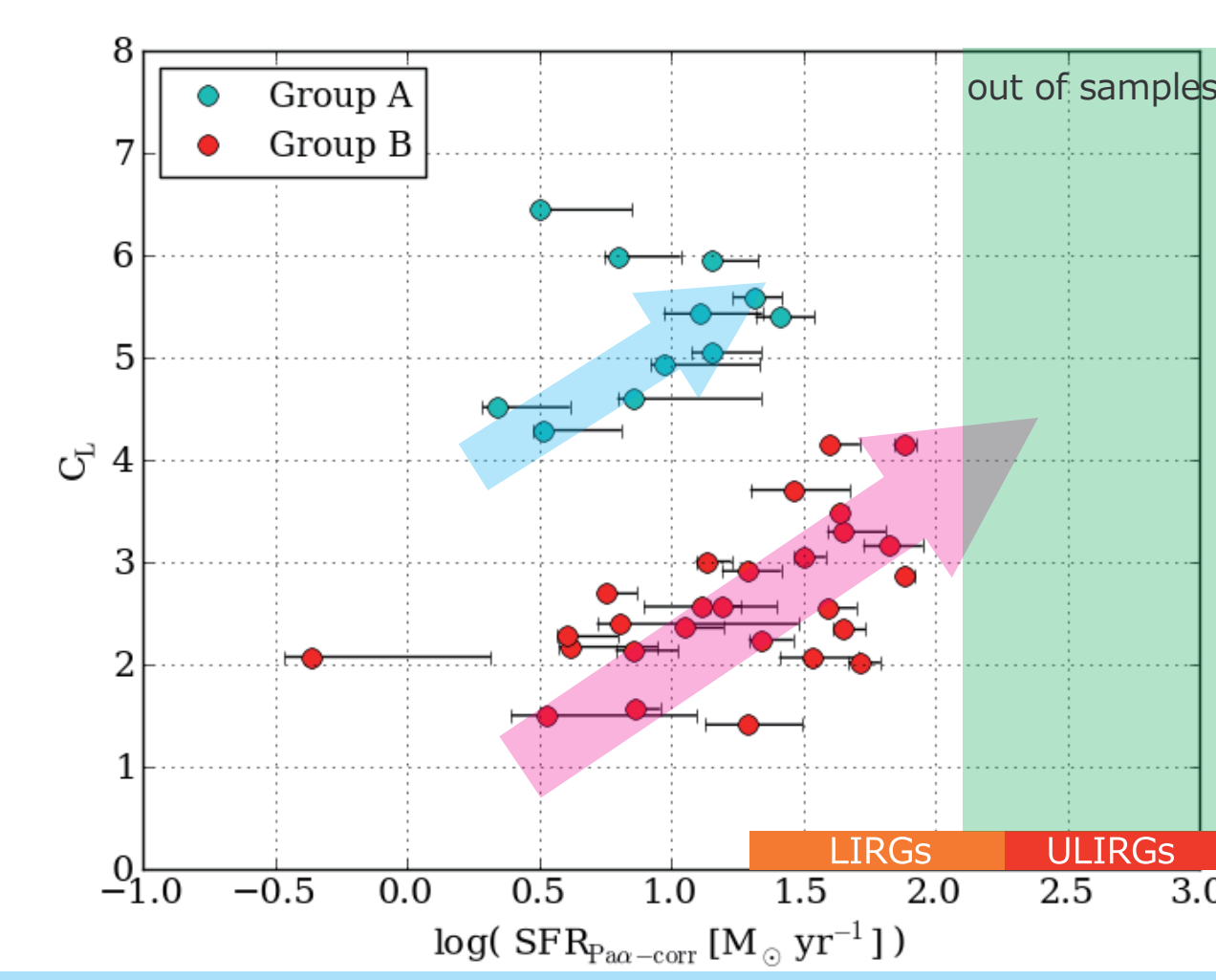


FIG.8 Comparison of CL and SFR

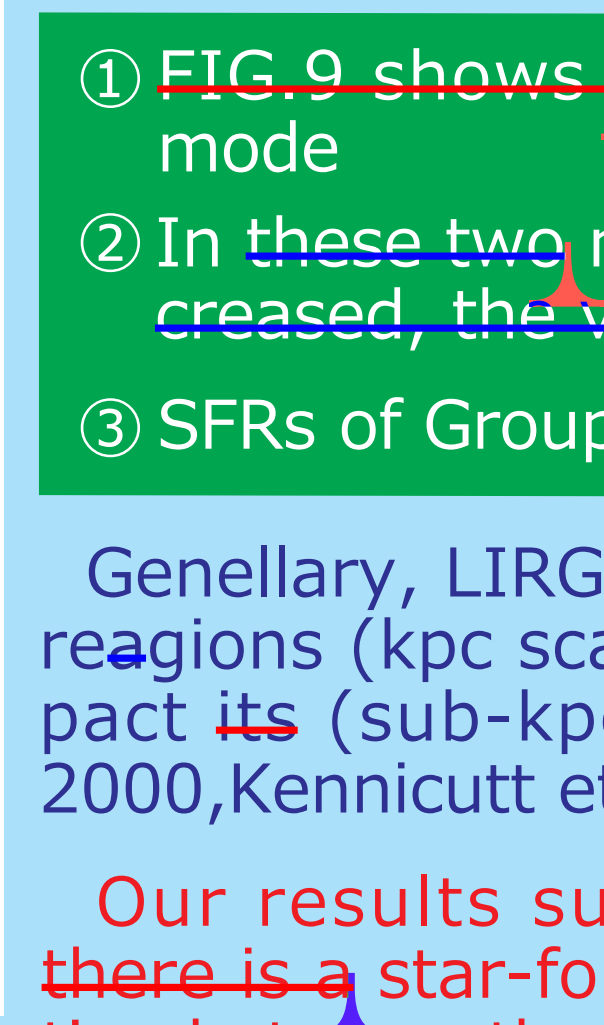


FIG.9 comparison of CL and C_L

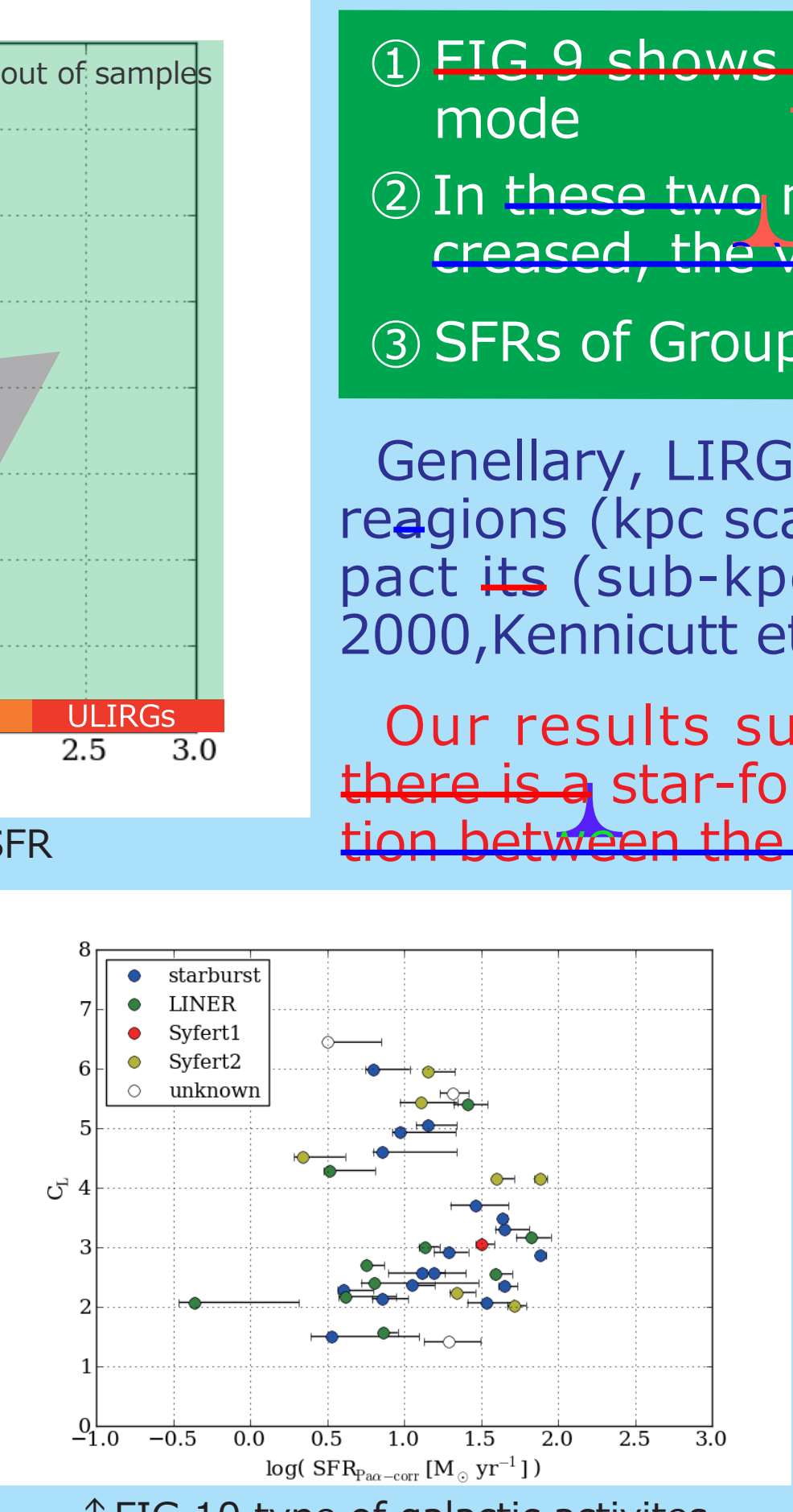


FIG.10 type of galactic activities

High C-Index

Low C-Index

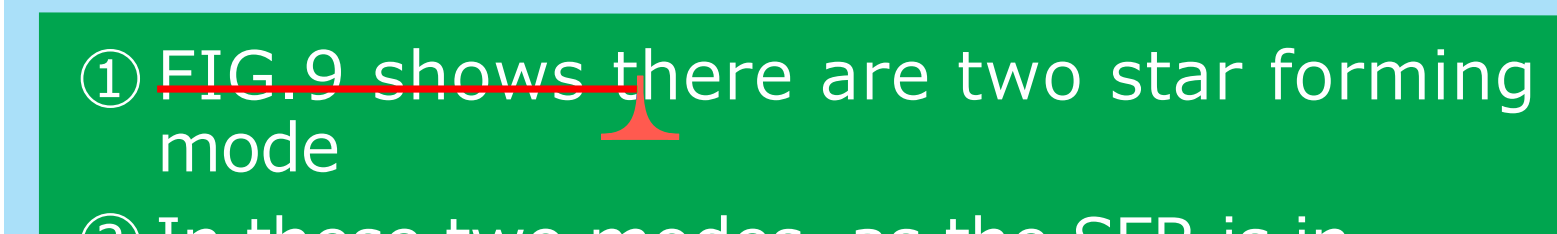


FIG.7 Two cases of C-Index.

- FIG.9 shows there are two star forming mode
- In these two modes, as the SFR is increased, the value of C_L is increased.
- SFRs of Group-A < 30 $M_{\odot} \text{ yr}^{-1}$

Genellary, LIRGs have diffused star forming reagions (kpc scale), and ULIRGs have compact its (sub-kpc scale) (e.g., Soifer et al. 2000, Kennicutt et al. 2009).

Our results suggests quantitatively that there is a star-forming region profile connection between the LIRGs and ULIRGs.

FIG.10 is the same as FIG.8, but it is color-coded according to the differences of some types of galactic activities, we can't find the features about FIG.10.